Front. Optoelectron. China 2010, 3(4): 370–375
DOI 10.1007/s12200-010-0120-y

RESEARCH ARTICLE

An analog notch filter for piezoelectric optical scanner

Xin WU (✉)[1], Sihai CHEN[1,2], Xiaogang XIONG[1], Benyi SHI[1], Wei CHEN[1]

1 College of Optoelectronic Science and Engineering, Huazhong University of Science and Technology, Wuhan 430074, China
2 Wuhan National Laboratory for Optoelectronics, Wuhan 430074, China

Abstract The optical scanner is one of the most important components in free-space optical communications, airborne and space-based lidars, adaptive optics, and so on. The performance of an optical scanner is frequently limited by the presence of mechanical resonances. This paper presents an analog notch filter with adjustable function to reject the mechanical resonances of the optical scanner. First of all, the structure and work principle of the piezoelectric optical scanner are introduced. Furthermore, the frequency sweep method based on virtual instruments is used to gain the natural frequency of the piezoelectric optical scanner. Then, the notch filters in series are used to reduce the oscillation of the scanner at the resonance frequencies. A variety of scanning experiments were carried out. After the introduction of the notch filter, the non-linearity was reduced to ±1.1% from ±2.1%. The linearity performance was greatly improved.

Keywords piezoelectric optical scanner, mechanical resonance, swept-sine waveform generator, notch filters, scan non-linearity

1 Introduction

Laser scanning technology is a technology which makes laser beams deflect, move, and scan. The device achieving laser scanning is called a laser scanner. Many types of scanners, such as galvanometer scanners, rotating mirror scanners, fast steering mirrors (FSMs) driven by piezoelectric actuators or voice coil actuators, are developed for laser scanning. Rotating mirror scanners have high resonance frequencies and large deflection angles, however, non-linearity errors caused by the radius difference and pyramid errors caused by non-parallelism of each plane limit their applications [1]. Galvanometer scanners are used in many scanning systems, but they cannot work at high frequency [2]. FSMs driven by voice coil actuators usually have large deflection angles but they have low resonance frequencies and high power consumption [3]. Traditional FSMs driven by piezoelectric actuators usually have high resonance frequencies but they have small deflection angles [4].

An optical tip-tilt actuator based on amplified piezoelectric actuators (APAs) was developed by Claeyssen et al. [5–8]. It has a resonance frequency of more than 1 kHz and a mechanical scan angle with 12 mrad. The scan angle is larger than that of traditional piezoelectric-actuated FSMs due to the special structure of the tip-tilt actuator. In most cases, the scanning system needs a laser scanner with characteristics such as fast linear scanning, small size and a small rotational inertia moment. A laser scanner driven by APAs has also been designed.

Many factors impact the linearity of the piezoelectric optical scanner. Hysteresis non-linearity is the major limitation in open-loop operation of piezoceramic actuators used in high-precision displacement applications. Many techniques have been designed to compensate for the hysteresis, such as the generalized preisach model [9]. This paper does not describe these methods in detail. After compensating for the hysteresis, the high-order harmonics near mechanical resonance frequencies which will excite oscillations of the scanner become the major factors that affect the scan linearity. The linearity performance of the piezoelectric optical scanner is frequently limited by the presence of mechanical resonance [10].

To summarize, the basic problem herein is to reduce the oscillation of the scanner system at the resonance frequencies. In this paper, an analog notch filter has been designed to solve this problem.

2 System design of piezoelectric optical scanner

The piezoelectric laser scanner consists of the components shown in Fig. 1(a): base, elastic shell, piezoelectric ceramic stack, resistance strain gauge, elastic hinge support and mirror. The APA is made up of the elastic shell and

Received July 21, 2010; accepted August 20, 2010

E-mail: laser_hust@foxmail.com

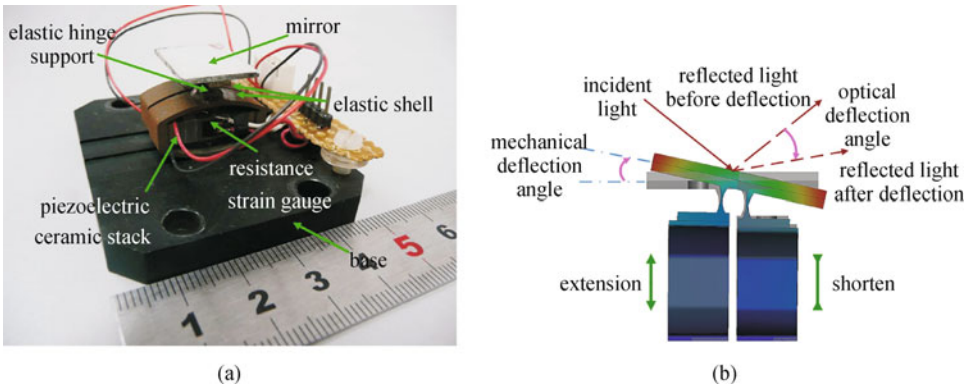

Fig. 1 Piezoelectric scanner. (a) Structure; (b) work principle

piezoelectric ceramic stack. The mirror is bounded at the top plane of the symmetrical elastic hinge support which is bolted on one side of the two elastic shells using screws. The other side of the two elastic shells is fixed to the base. The elastic shell can be used to prestress piezoelectric ceramic stacks and prevent ceramics from working in tensile stress. Resistance strain gauges are bounded at the outside of each piezoelectric ceramic stack.

The schematic structure of the piezoelectric laser scanner is shown in Fig. 1(b). The two piezoelectric ceramic stacks can extend to the same length by applying the same voltage. The displacement on contraction is several times larger than extension. The opposite voltage can make the stacks do the opposite movement so that the mirror on the top plane of the flexure support rotates around the axis. The displacement amplification and the parallel arrangements provide a larger tilt angle than the traditional piezoelectric-actuated scanners. The resistance strain gauge and external circuit resistance constitutes a bridge circuit. Voltage difference is created when the voltage applied to one APA increases and to another APA decreases. The difference can indirectly reflect the angle change of the piezoelectric laser scanner.

3 Performance testing of laser scanner

A block diagram of the performance test bench is shown in Fig. 2(a). The static and dynamic performances of the laser scanner are measured on the test bench (Fig. 3). In the performance testing, the system's input is the voltage wave generated by the wave generator, and the system's output is the deflection angle of the scanner. The control circuit is not used in the static and dynamic performance tests, but it is used to improve the scanning linearity of the laser scanner. The scanning linearity is different from that in static performances, and it is the linearity of the scanned path at linear scanning. It reveals the extent of deviation of the scanned path to the estimated triangle waveform path. The scanning linearity changes according to the scanning frequency. The relation of optical deflection angle and the driving voltage is shown in Fig. 3(a). As can be seen in Fig. 3(a), the hysteresis behavior of the piezoelectric ceramic is obvious and it will affect the scanning linearity of the laser scanner.

The scanning non-linearity of a point in the scanning waveform is defined in Fig. 3(a). The definition of the scanning non-linearity is

$$N_{\text{nonl A}} = \frac{\Delta\theta}{\theta_{\max}}, \tag{1}$$

where $\theta_{\max}$ is the maximum optical deflection angle.

The frequency sweep method based on virtual instruments is used to gain the natural frequency of the piezoelectric optical scanner (Fig. 2(b)). Swept sine waves are useful when we want to test a product over a wide frequency range [11]. We create a swept sine function in the National Instruments' LabView with one VI (virtual instrument). The LabView frequency sweep program gradually increases the clock frequency of the system, and the output frequency of the data acquisition card will gradually increase. The LabView software calculates an array of numbers that represent the swept-sine-wave time series at each sample point as the frequency increases. The frequency change of the output must be handled on a point-by-point basis. Swept sine waves are used to test the piezoelectric optical scanner over a wide frequency range. The magnitude-frequency response of the piezoelectric optical scanner is obtained through another LabView acquisition program. The magnitude-frequency response reveals that the primary resonance frequencies are the first two resonance frequencies, which are 2000 and 2445 Hz, respectively (Fig. 3(b)).

4 Notch filter design for piezoelectric optical scanner

The triangle wave is composed of many high order harmonics. The Fourier series of a triangle wave is given as

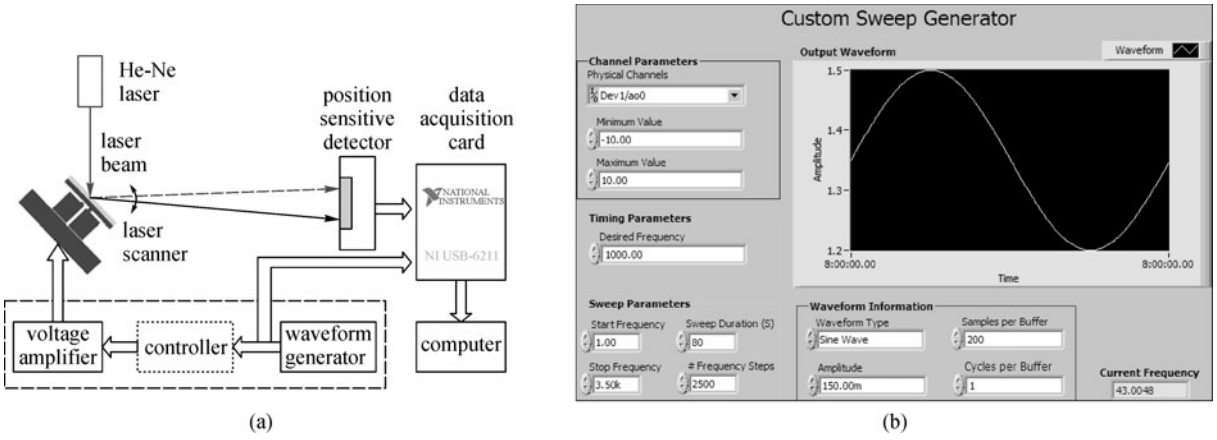

Fig. 2 Block diagram. (a) Performance test bench; (b) swept-sine waveform generator

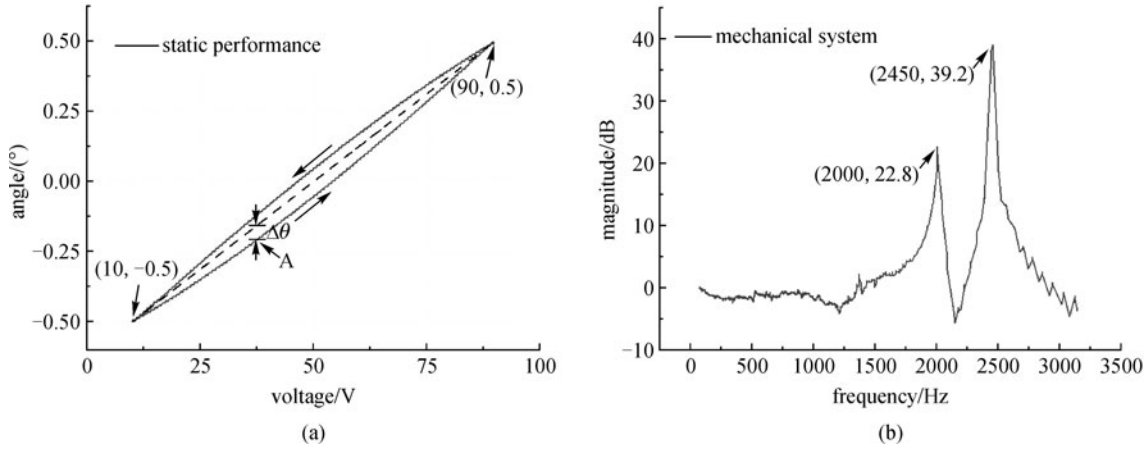

Fig. 3 Piezoelectric optical scanner. (a) Static performance; (b) dynamic performance

$$f(t) = \frac{E}{2} + \frac{4E}{(n\pi)^2}\sum_{n=1}^{\infty}\sin^2\left(\frac{n\pi}{2}\right)\cos(n\omega t), \qquad (2)$$

where E is the amplitude of the triangle wave.

The odd harmonics near mechanical resonance frequencies will excite oscillations of the laser scanner. If the frequency of the triangle wave frequency is above 50 Hz, the laser scanner starts to oscillate evidently due to its mechanical resonance. As shown in Fig. 3(b), the first two resonance frequencies are major influential factors on the oscillation. Two notch filters in series are used to reduce the oscillation amplitude of the scanner system at the first two resonance frequencies, thus reducing the oscillation. Because the resonance at the frequency of 2000 Hz degrades the linearity seriously, the stronger attenuation is needed here. Figure 4 is the schematic of the single notch filter used to reduce the oscillation [12]. This paper will describe its principles in detail.

From Fig. 4, functions of the circuit can be obtained from the ideal operational amplifier's two important characteristics, Kirchhoff's current law (KCL) and Kirchhoff's voltage law (KVL). Equations (3)–(7) are the Laplace transform of these functions:

$$\frac{V_{\text{in}}}{R_1} + \frac{V_3}{R_4} + \frac{V_1}{R_2} = 0, \qquad (3)$$

$$\frac{V_1}{R_3} + \frac{V_4}{R_6} + sV_2C_1 = 0, \qquad (4)$$

$$\frac{V_2}{R_5} + \frac{V_3}{R_7} = 0, \qquad (5)$$

$$\frac{V_3}{R_8} + sV_4C_2 = 0, \qquad (6)$$

$$V_{\text{out}} - \left(\frac{V_{\text{in}}R_9}{R_9 + R_{10}} + \frac{V_3R_{10}}{R_9 + R_{10}}\right)\left(1 + \frac{R_{12}}{R_{11}}\right) = 0, \qquad (7)$$

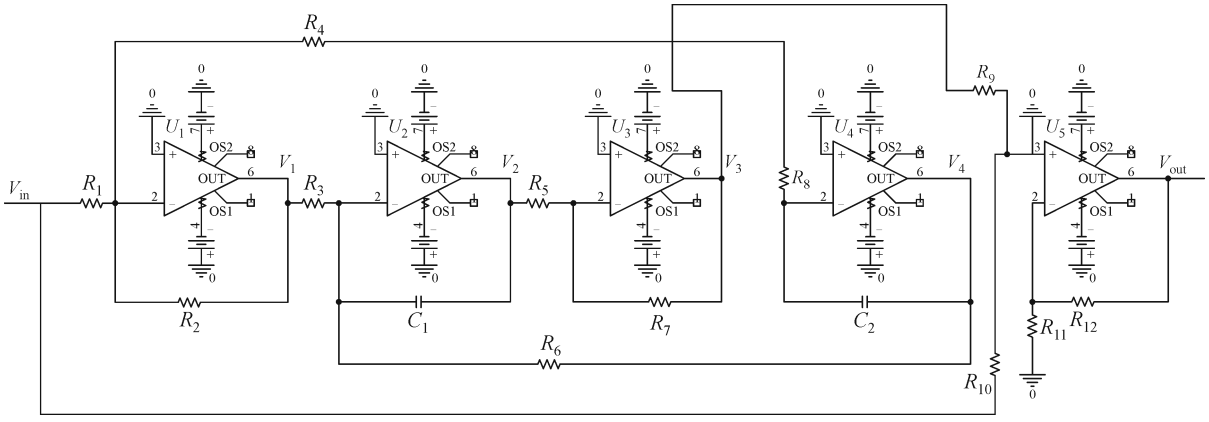

Fig. 4 Schematic of single notch filter

where $R_2 = 13\ \text{k}\Omega$, $R_3 = 65\ \text{k}\Omega$, $R_5 = R_7 = 50\ \text{k}\Omega$, $R_9 = R_{10} = R_{11} = R_{12} = 10\ \text{k}\Omega$, and $C_1 = C_2 = 79.575\ \text{pF}$. Substituting Eqs. (3)–(6) into Eq. (7) yields the transfer function of the circuit:

$$G(s) = \frac{V_{\text{out}}}{V_{\text{in}}} = \frac{s^2 + s\left(1 - \dfrac{R_4}{R_1}\right)\dfrac{\omega_0}{Q} + \omega_0^2}{s^2 + s\dfrac{\omega_0}{Q} + \omega_0^2}, \tag{8}$$

where ω_0 and Q are the characteristic angular frequency and equivalent quality factor of the circuit, respectively. The characteristic corner frequency, whose dimension unit is rad/s, and the equivalent quality factor are found as follows:

$$\omega_0 = \sqrt{\frac{1}{R_6 R_8 C^2}}, \tag{9}$$

$$Q = \sqrt{\frac{1}{R_6 R_8}}\frac{R_3}{R_2}R_4, \tag{10}$$

where $C = C_1 = C_2$. From Eq. (9), we can get the filter's center frequency, which is given by

$$f_0 = \frac{\omega_0}{2\pi} = \sqrt{\frac{1}{R_6 R_8}}\left(2 \times 10^9\right). \tag{11}$$

The unit of f_0 is Hz. For a different frequency, the parameter settings of R_6 and R_8 are different. Therefore, for 2000 Hz, the resistivity of R_6 and R_8 is 1000 kΩ, while for 2445 Hz, the resistivity of R_6 and R_8 is 818 kΩ. In the circuit, we use a variable resistor (R_6 and R_8) to fit the needs of different frequencies.

Substituting $s = \text{j}\omega$ into Eq. (8) gives

$$G(\omega) = \frac{\left(1 - \dfrac{R_4}{R_1}\right) + \text{j}Q\left(\dfrac{\omega}{\omega_0} - \dfrac{\omega_0}{\omega}\right)}{1 + \text{j}Q\left(\dfrac{\omega}{\omega_0} - \dfrac{\omega_0}{\omega}\right)}. \tag{12}$$

The formula above shows that the circuit is a notch filter. Notice that $G(0) = 1$, $G(\infty) = 1$. The transfer function of the notch filters in series is given as follows:

$$G(s) = G_1(s) \times G_2(s) = \frac{s^4 + 1256\ s^3 + 3.95 \times 10^8\ s^2 + 1.984 \times 10^{11}\ s + 3.745 \times 10^{16}}{s^4 + 5575\ s^3 + 4.027 \times 10^8\ s^2 + 1.123 \times 10^{12}\ s + 3.745 \times 10^{16}}. \tag{13}$$

We can obtain the magnitude-frequency characteristic of the circuit by plotting the magnitude of the transfer function as the frequency varies. The magnitude of $G(s)$ is

$$20\log_{10}\left|\frac{G(\omega)}{G_0}\right| = 20\log_{10}\left|\frac{\left(1 - \dfrac{R_4}{R_1}\right) + \text{j}Q\left(\dfrac{\omega}{\omega_0} - \dfrac{\omega_0}{\omega}\right)}{1 + \text{j}Q\left(\dfrac{\omega}{\omega_0} - \dfrac{\omega_0}{\omega}\right)}\right|. \tag{14}$$

Figure 5(a) shows the magnitude plot of the transfer function. From Fig. 5(a), we can find that the results of the center frequency and the attenuation are originally envisaged.

Figure 5(a) is an ideal situation in which all resistors have no error. Substituting $\omega = \omega_0$ into Eq. (14), we can find the gain at the center frequency by finding the magnitude of the transfer function at ω_0, as

$$20\log_{10}\left|\frac{G(\omega_0)}{G_0}\right| = 20\log_{10}\left|1 - \frac{R_4}{R_1}\right|. \tag{15}$$

The larger attenuation is needed for 2000 Hz, so resistor R_1 and R_4 should both be 1000 kΩ. For 2450 Hz, resistor R_1 and R_4 should be 2000 and 1000 kΩ, respectively.

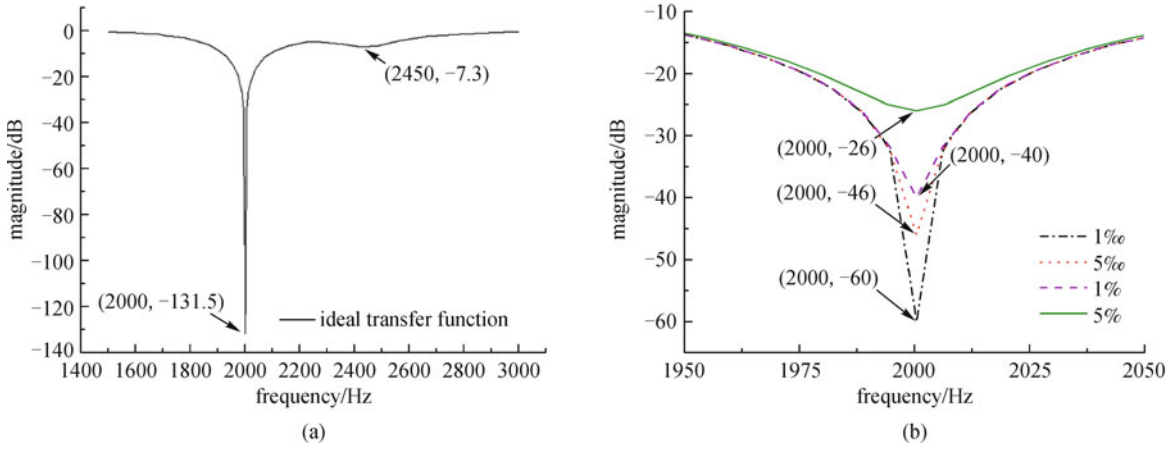

Fig. 5 Ideal transfer function. (a) Magnitude-frequency characteristic; (b) resistance difference impact on the gain at center frequency

If R_1 needs to be equal to R_4, corresponding to 2000 Hz, we find that the gain at the center frequency ω_0 is impacted by the resistance nuances between R_1 and R_4. Resistor tolerance is assumed as P. If the resistance tolerance P is 1‰, then $|1-R_4/R_1|$ will be 0.001. We can get that the gain at the center frequency will be -60 dB. If the resistance tolerance P is 0.005, then $|1-R_4/R_1|$ will be 0.005. The gain at the center frequency will be -46 dB. As shown in Fig. 3, the absolute value of the gain decreases when the resistance difference increases. In order to get a large attenuation at the center frequency, we should strictly filter the resistance.

5 Experimental results

PSpice is a useful tool for obtaining the frequency response of circuits. The frequency response is obtained using the AC Sweep. We let the input voltage V_{in} be a sinusoid of amplitude 1 V. After simulating the circuit, we set the probe window to display the plots of $20\log_{10}(V_{out}/V_{in})$, as shown in Fig. 6(a). Notice that the plots in Fig. 6(a) are similar to those in Fig. 5(a). The simulation results comply with the principles analyzed above.

Notch filters described in Fig. 4 are implemented in hardware circuits. The magnitude-frequency response of the notch filter is also obtained through the same method as mentioned above. The magnitude-frequency characteristics of the notch filter tested is shown in Fig. 6(b). We find that the center frequencies of the two notches are slightly offset because of the resistance tolerance of R_6 and R_8. Besides the offset, the first two resonance frequencies are obviously restrained by the filter.

We carried out a variety of frequency scanning experiments. Scanning waveforms and non-linearities with and without notch filters at 100 Hz is shown as Fig. 7. Because of the existence of the resonance frequencies, non-linearity was still around $\pm 2.2\%$ after hysteresis compensation. It remained as the shortcoming for the situation which required high linearity. After the introduction of notch filters, the amplitude of the scanner system at the resonance frequencies was restrained and the

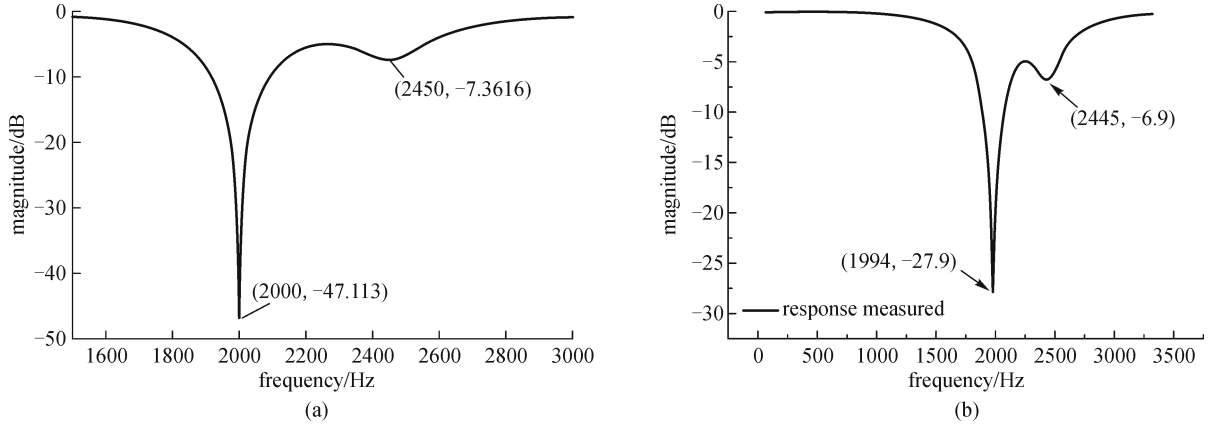

Fig. 6 Notch filter in series. (a) Pspice simulation result; (b) magnitude-frequency characteristics measured

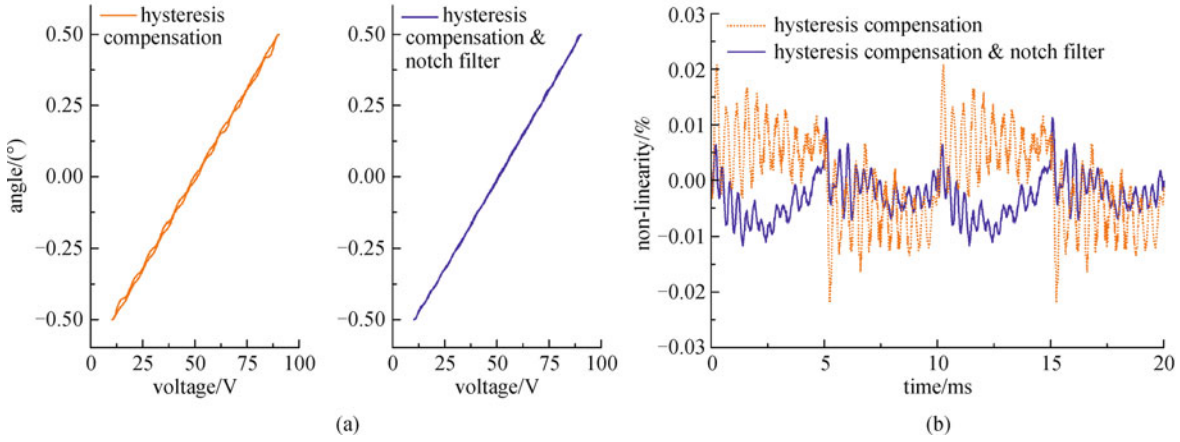

Fig. 7 Hysteresis compensated laser scanner with and without notch filters at linear scanning of 100 Hz. (a) Scanning waveforms; (b) non-linearities

non-linearity was reduced to ±1.1%. The linearity performance was greatly improved.

6 Conclusion

In this paper, a compact optical scanner which is based on a pair of amplified piezoelectric actuators is designed. The test results show that the laser scanner has high mechanical resonance frequencies. The factors influencing the scanning linearity are analyzed.

A notch filter has been designed to restrain the oscillations that are caused by the mechanical resonances of the scanner after compensating for the hysteresis by a feed-forward controller. The piezoelectric scanner described in this paper has been greatly improved compared to a traditional piezoelectric scanner. There is a wide range of applications of the method in suppressing mechanical resonances not only in the field of piezoelectric optical scanners.

The scanner also has other advantages, such as low moment of inertia, small size, simple structure, and low power consumption.

Acknowledgements This work was supported by the Program for New Century Excellent Talents in University of China (No. NCET-07-0319).

References

1. Xu M, Hu J S. Analysis and calculation of rotating polygonal scanner in laser scanning imaging system. Chinese Journal of Lasers, 2008, 35(5): 782–787 (in Chinese)
2. Wang X Q, Liao S, Hung J M. Study on the amplitude-frequency performance testing and position demarcating of optical scanner. Opto-Electronic Engineering, 2004, 31(z1): 73–79 (in Chinese)
3. Wu Q Y, Wang Q, Peng Q, Ren G, Fu C Y. Wide bandwidth control of fast-steering mirror driven by voice coil motor. Opto-Electronic Engineering, 2004, 31(8): 15–18 (in Chinese)
4. Ling N, Chen D H, Guan C L. Two-dimensional piezoelectric fast steering mirror. Opto-Electronic Engineering, 1995, 22(1): 51–60 (in Chinese)
5. Claeyssen F, Le Letty R, Barillot F, Lhermet N, Fabbro H, Guay P, Yorck M, Bouchilloux P. Mechanisms based on Piezo actuators. Proceedings of SPIE, 2001, 4332: 225–233
6. Bouchilloux P, Claeyssen F, Le Letty R. Amplified piezoelectric actuators: from aerospace to underwater applications. Proceedings of SPIE, 2004, 5388: 143–154
7. Claeyssen F, Lhermet N, Le Letty R, Barillot F, Debarnot M, Six M F, Thomin G, Privat M, Bouchilloux P. Piezoelectric actuators and motors based on shell structures. Proceedings of SPIE, 2000, 3991: 202–209
8. Le Letty R, Claeyssen F, Lhermet N, Bouchilloux P. New amplified piezoelectric actuator for precision positioning and active damping. Proceedings of SPIE, 1997, 3041: 496–504
9. Ge P, Musa J. Generalized Preisach model for hysteresis nonlinearity of piezoceramic actuators. Precision Engineering, 1997, 20(2): 99–111
10. Li X Y, Ling N, Chen D H, Yu J L. Stable control of the fast steering mirror in adaptive optics system. High Power Laser and Particle beams, 1999, 11(1): 31–36 (in Chinese)
11. McPeak S. Create a swept-sine function in LabView with just one virtual instrument. EDN, 2009, June 25: 43–52
12. Maxim. 4th- and 8th-order continuous-time active filters. Maxim Integrated Products, 1996, 19-4191: 11–17